Pergamon

Int. J. Heat Mass Transfer. Vol. 41, No. 2, pp. 253–260, 1998

Printed in Great Britain
0017–9310/98 $19.00+0.00

PII: S0017–9310(97)00151–8

Minimum thickness of a liquid film flowing down a vertical tube

D. T. HUGHES

Department of Chemical and Process Engineering, University of Surrey, Guildford, Surrey GU2 5XH, U.K.

and

T. R. BOTT

School of Chemical Engineering, University of Birmingham, P.O. Box 363, Birmingham, B15 2TT, U.K.

(*Received* 22 *May* 1997)

Abstract—In processing equipment in which falling films are employed, the break up of the film may be a limitation on the effective use of the surface for transfer operations. A model has been developed which enables the geometry of fluids travelling down the inside or outside of vertical tubes to be calculated. Once the geometry of the film or rivulet flow has been found, the associated heat or mass transfer conditions can be calculated. Flow geometries can be calculated for any flowrate and it is expected that this theory will be of value in the optimisation of falling film equipment. © 1997 Elsevier Science Ltd.

1. INTRODUCTION

When a liquid flows down a vertical tube at a low flowrate it may not be able to completely cover the tube surface. The flow will comprise a number of rivulets separated by unwetted areas or dry patches. Predictions of the critical flowrate (F_*), below which it is not possible to maintain film flow, may be needed in the analysis of heat and mass transfer equipment in order to optimise the plant economics. With the increasing interest in the use of low cost, low surface energy materials such as plastics, relatively high flowrates are required to wet fully the tubes. In these systems, the ability to be able to calculate the minimum wetting rate becomes more important, as the use of high flowrates will usually result in significant pumping costs.

In some theoretical studies of film breakdown, the analysis starts by study of a force balance at the point of liquid stagnation at the upstream point of a dry patch [1]. In other studies the energies of film and rivulet flows are examined, and it is assumed that a stable flow configuration will exist at the minimum of the total energy function [2, 3]. Much work has been done on the hydrodynamics of rivulet flow [4, 5]. Also, models have been presented in which the equilibrium configuration of liquids flows are calculated [6], and the behaviour of meandering rivulets has been investigated [7].

In this paper, a model describing the flow of films and rivulets down vertical tubes is presented. This work is based on the model of Mikielewicz and Moszynski [3] in which the minimum thickness of a liquid film flowing down a plane solid surface is calculated. There are three significant advantages of the present theory. These are:

(1) The flows considered are flows down either the inside or outside of tubes. Previous models consider infinitely wide flat surfaces. By taking the tube curvature into account the present theory is directly relevant to many plant processes.

(2) The type of flow (film/rivulet) adopted by the system can be calculated for any flowrate. With the present calculation procedure, the process heat or mass transfer conditions (that follow from the calculated flow configurations) may be evaluated over the complete flow range. This is particularly important for industrial processes for which a plant optimisation study is required.

(3) The assumption that rivulet flows (inside or outside the tube) should be made up of congruent rivulets is not required. The present theory is, therefore, completely general. However, the assumption of identical rivulet geometries reduces computing times significantly.

The procedures presented in the following sections for the calculation of rivulet/film fluid flow and heat transfer characteristics are numerically exact and have been developed from an approximate calculation sequence previously presented by the authors [8]. As in the previous paper, the results of the film and rivulet model are used to examine the experimental results obtained from experiments in which water was evaporated as it travelled down the inside of a 6 mm diam-

NOMENCLATURE

a	constant
A	area
b	constant
c	constant
C_1, C_2, C_3	constants
e	element number
E	energy per unit length
f	rivulet flowrate
F	total flowrate
g	acceleration due to gravity
h	heat transfer coefficient
k	thermal conductivity
L	natural coordinate
M	number of different rivulet angles
n	number of rivulets
n_1	number of elements
n_0	outward normal
N	shape function
P	maximum number of rivulets in tube
r	distance from tube axis
R	tube radius
S	radius of curvature of rivulet
T	temperature
T_0	external temperature
ΔT	temperature difference
U	overall heat transfer coefficient
w	fluid velocity down tube
x	cartesian coordinate
y	cartesian coordinate
z	cartesian coordinate
Z	number of distinct flow configurations.

Greek symbols

α	half angle subtended by rivulet at tube axis
β	angle (Fig. 1)
γ	surface tension
δ_0	film thickness
δ_w	thickness of tube wall
δ_*	critical film thickness
θ	contact angle
μ	liquid viscosity
ν	rivulet number
ρ	liquid density.

Subscripts

g	gas
i	node label
j	node label
k	node label
K	kinetic
l	liquid
s	solid
T	total
w	wall
X	for wetted parts of tube
σ	surface
*	critical.

Superscript

(e)	element.

eter nylon-12 tube of wall thickness 150 μm. The experimental programme which generated these results was initiated to study the feasibility of the use of plastic tubes in vapour recompression falling film evaporators [9–11].

2. FLOW MODELS

The liquid flow down the tube may comprise a number of rivulets or a continuous film. For a given flowrate, the configuration adopted is decided by considering the total (surface and kinetic) energy of all the possible flow configurations in which the system can exist. The configuration adopted is then assumed to be the configuration with the lowest energy. This approach can be used to examine flow systems both inside and outside the tube. In this section, expressions are obtained for the flowrate, surface energy and kinetic energy of the flows.

2.1. *Film flow*

The energies per unit length of liquid films of thickness δ_0 flowing down the inside and outside of a tube are calculated. When considering flows down the inside of a tube, the inside diameter of the tube is taken to be $2R$. For external flows, the outside diameter of the tube, cylinder or wire is taken to be $2R$.

A cylindrical polar coordinate system is used in which the film flows at a velocity w in the direction of the z-axis. The z-axis is coincident with the tube axis and is the direction in which gravity acts. Under steady state conditions, there is no flow in a plane perpendicular to the z-axis and the Navier–Stokes equations reduce to

$$\frac{1}{r}\frac{\partial}{\partial r}\left(r\frac{\partial w}{\partial r}\right)+\frac{\rho g}{\mu}=0. \tag{1}$$

Equation (1) can be integrated with the film boundary conditions.

$$w = 0 \quad \text{when } r = R$$

and

$$\frac{\partial w}{\partial r} = 0 \quad \text{when } r = C_1$$

where

$$C_1 = R-\delta_0 \text{ for internal flows}$$

and

$$C_1 = R+\delta_0 \text{ for external flows.}$$

This gives the film velocity profile

$$w = \frac{\rho g}{2\mu}\left[C_1^2 \ln\frac{r}{R} + \frac{R^2-r^2}{2}\right]. \tag{2}$$

The volume rate of flow down the tube (F) is given by

$$F = \int_{C_3}^{C_2} 2\pi w r \, dr$$

$$= \frac{\pi\rho g}{8\mu}\left[4r^2C_1^2 \ln\frac{r}{R} + 2R^2r^2 - 2C_1^2r^2 - r^4\right]_{C_3}^{C_2} \tag{3}$$

where for internal flows $C_2 = R$ and $C_3 = R-\delta_0$. For external flows $C_2 = R+\delta_0$ and $C_3 = R$.

The kinetic energy of the film per unit length of tube is given by

$$E_K(\text{film}) = \int_{C_3}^{C_2} \pi\rho w^2 r \, dr$$

$$= \frac{\pi\rho^3 g^2}{4\mu^2}\left[\frac{C_1^4r^2}{2}\left(\ln\frac{r}{R}\right)^2 - \frac{C_1^4r^2}{2}\ln\frac{r}{R} + \frac{C_1^4r^2}{4} + \frac{R^2C_1^2r^2}{2}\ln\frac{r}{R} - \frac{R^2C_1^2r^2}{4} - \frac{C_1^2r^4}{4}\ln\frac{r}{R} + \frac{r^4C_1^2}{16} + \frac{R^4r^2}{8} - \frac{r^4R^2}{8} + \frac{r^6}{24}\right]_{C_3}^{C_2}. \tag{4}$$

The surface energy per unit length of the system is given by

$$E_\sigma(\text{film}) = 2\pi R\gamma_{ls} + 2\pi C_1\gamma_{lg}. \tag{5}$$

The total energy of the system per unit length of tube is given by

$$E_T = E_K + E_\sigma. \tag{6}$$

Combining equations (5) and (6) gives

$$E_T - 2\pi R\gamma_{ls} = E_K(\text{film}) + 2\pi C_1\gamma_{lg}. \tag{7}$$

The left-hand side of equation (7) is the total energy of the system minus a constant and is the function that is used to compare the relative energies of the film and rivulet configurations.

2.2. *Rivulet flow*

As in the theory of Mikielewicz and Moszynski [3], the surface of the rivulet is taken to be a segment of a circle. This is consistent with uniform surface tension. The rivulet contacts the tube surface at an angle θ (the contact angle) and subtends an angle 2α at the centre of the tube. Four types of rivulet can be distinguished and these are shown in Fig. 1. For external flows the rivulets are always concavoconvex. For internal flows, there are three possibilities for the rivulet geometry. If α is greater than θ, then the rivulet is concavoconvex. If α equals θ, a planoconvex rivulet exists and if θ exceeds α, the rivulet is biconvex. The radius of curvature of the tube surface is R and for all rivulet types except planoconvex, the rivulet surface is part of a circle of radius S. From Fig. 1, it can be seen that the following relations exist between α, β and θ.

External concavoconvex rivulet

$$\theta = \beta-\alpha. \tag{8a}$$

Internal concavoconvex rivulet

$$(\alpha > \theta) \quad \theta = \alpha-\beta. \tag{8b}$$

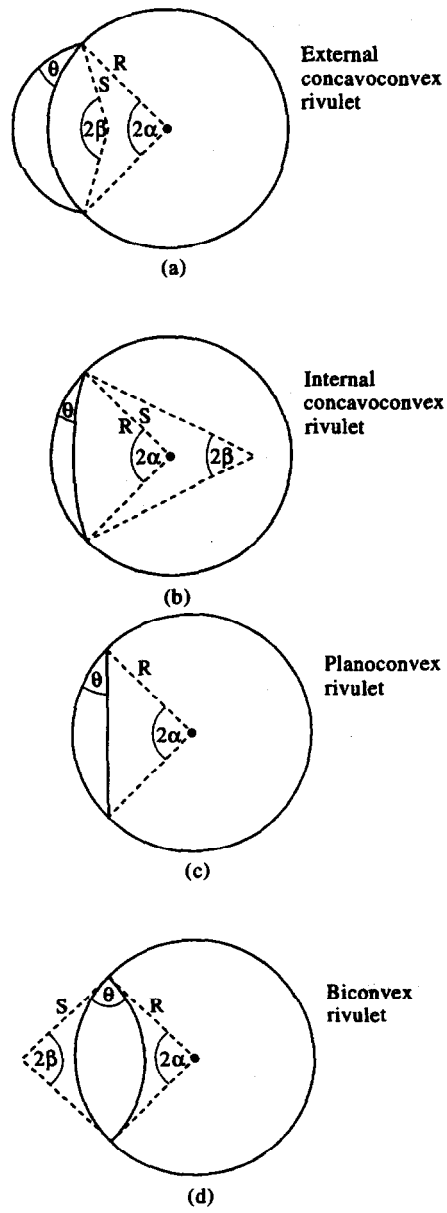

Fig. 1. Rivulet geometries.

Planoconvex rivulet

$$(\alpha = \theta).$$

Biconvex rivulet

$$(\theta > \alpha) \quad \theta = \alpha + \beta. \tag{8c}$$

For all rivulets except planoconvex

$$S \sin \beta = R \sin \alpha. \tag{9}$$

For a given tube radius (R) the rivulet is completely defined by the known value of θ and the selected value of α. The corresponding values of β and S may be calculated from equations (8) and (9) above. The velocity distribution in the rivulet is obtained numerically using the finite element method [12].

A cartesian coordinate system (x, y, z) is used in which the rivulet flows at a velocity w in the direction of the z-axis. Under steady state conditions in which there is no flow in a plane perpendicular to the z-axis, the Navier–Stokes equations reduce to

$$\frac{\partial^2 w}{\partial x^2} + \frac{\partial^2 w}{\partial y^2} + \frac{\rho g}{\mu} = 0. \tag{10a}$$

This equation is solved subject to the boundary conditions

$$w = 0 \quad \text{at the tube wall} \tag{10b}$$

and

$$\frac{\partial w}{\partial n_0} = 0 \quad \text{at the free surface of the rivulet} \tag{10c}$$

where n_0 is the outward normal to the free rivulet surface.

The rivulet is meshed using three-noded triangular elements and, because of symmetry, only half the rivulet is modelled. A schematic diagram of an internal rivulet is shown in Fig. 2. The finite element code used for the calculations was written in FORTRAN. From the calculated nodal velocities, the rivulet flowrates and kinetic energies were calculated.

The fluid velocity down the tube at any point in an element, $w^{(e)}$ is given by

$$w^{(e)}(x, y) = N_i w_i + N_j w_j + N_k w_k \tag{11}$$

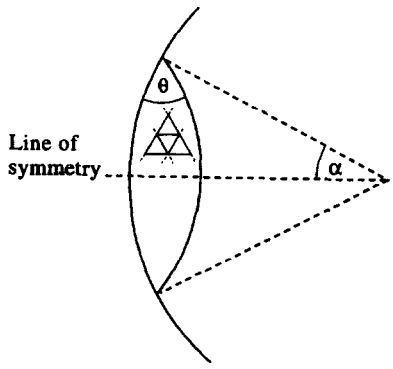

Fig. 2. Meshing of half the rivulet using three-noded elements.

where N are the element shape functions with the three subscripts i, j, k referring to each of the nodes. The total flowrate for each rivulet is given by

$$f = \sum_{e=1}^{n_1} \iint w^{(e)} \, dA. \tag{12}$$

Using the expression [12]:

$$\iint_A L_i^a L_j^b L_k^c \, dA = \frac{a!b!c!}{(a+b+c+2)!} 2A \tag{13}$$

where the natural coordinates L are identical to the shape functions N, the rivulet flowrate can be obtained from equations (11) and (12) as

$$f = \frac{1}{3} \sum_{e=1}^{n_1} A^{(e)} [w_i + w_j + w_k]. \tag{14}$$

The kinetic energy of the rivulet per unit length of tube is given by

$$E_K = \sum_{e=1}^{n_1} \iint \frac{1}{2} \rho [w^{(e)}]^2 \, dA \tag{15}$$

using equations (11) and (13), equation (15) may be expressed as

$$E_K = \frac{1}{6} \sum_{e=1}^{n_1} A^{(e)} [w_i^2 + w_j^2 + w_k^2 + w_i w_j + w_j w_k + w_k w_i] \frac{\rho}{2}. \tag{16}$$

If the flow configuration travelling down the tube is made up of n rivulets, in which the vth rivulet subtends an angle $2\alpha_v$ at the tube axis, the total energy of the system can be written as

$$E_T = \sum_{v=1}^{n} [E_K]_v + 2R\gamma_{sl} \sum_{v=1}^{n} \alpha_v + 2\gamma_{lg} \sum_{v=1}^{n} \beta_v S_v + 2R\gamma_{sg} \left[\pi - \sum_{v=1}^{n} \alpha_v \right]. \tag{17}$$

Using Young's equation [13, 14]:

$$\gamma_{sg} = \gamma_{sl} + \gamma_{lg} \cos \theta \tag{18}$$

it follows that equation (17) can be rewritten as

$$E_T - 2\pi R\gamma_{sl} = \sum_{v=1}^{n} [E_K]_v + 2\gamma_{lg} \sum_{v=1}^{n} \beta_v S_v + 2R\gamma_{lg} \cos \theta \left[\pi - \sum_{v=1}^{n} \alpha_v \right]. \tag{19}$$

Also, the total flowrate down the tube is given by

$$F = \sum_{v=1}^{n} f_v. \tag{20}$$

Equations (19) and (20) are general expressions for the rivulet configuration flowrate and energy. If it is assumed that the rivulets are congruent, equations (19) and (20) become

$$E_T - 2\pi R\gamma_{sl} = nE_K + 2n\gamma_{lg}\beta S + 2R\gamma_{lg}\cos\theta[\pi - n\alpha] \quad (21)$$

and

$$F = nf. \quad (22)$$

3. PREDICTIONS FROM THEORY

The theory of the previous section is used to model the evaporation of demineralised water at 100°C flowing down the inside of a 6 mm nylon-12 tube with a water-tube contact angle of 50°. These values for the water temperature, tube diameter ($2R$) and contact angle (θ) have been chosen because they represent the parameters of a system for which experimental results are available [8]. In the experiment, the heat for the evaporation of the water was provided by steam condensing on the outside of the nylon tube of wall thickness 150 μm. The tube length was 4.15 m and the log mean temperature difference across the dropwise condensate, tube wall and demineralised water was 0.52°C.

3.1. *Calculation of the fluid geometry*

Using the flow and energy equations for internal film flow (3) and (7), together with the equations for internal rivulet flow, (21) and (22), in which the rivulets are assumed to be congruent, a graph of relative energy per unit length of tube vs flowrate is constructed. The mode of flow for any given flowrate is then decided by referring to the graph and choosing the configuration which has the lowest relative energy.

The tube radius is set at 3 mm and the appropriate values of γ_{ls}, ρ and μ for 100°C water are chosen. The water–plastic contact angle θ is 50°.

3.1.1. *Film flow.* Values of δ_0 over the range 0–200 μm are chosen and substituted into equations (3) and (4) to give values of F and E_K. This then allows calculation of $E_T - 2\pi R\gamma_{ls}$ from equation (7). The resulting pairs of values for energy and flowrate may be plotted on a graph.

3.1.2. *Rivulet flow.* In these calculations for the plastic tube–water system, the rivulets are all found to be biconvex, i.e. $\theta > \alpha$. For biconvex rivulets, the value of β can be calculated from the known value of θ and assumed value of α using equation (8c). The corresponding value of the rivulet radius of curvature may then be found from equation (9). From the values of θ, α and R the rivulet geometry is completely defined.

Half the rivulet was meshed using 400 three-noded triangular elements (Fig. 2) and the Poisson equation (10a) was solved for the flow down the tube subject to the boundary conditions (10b) and (10c). Checks to ensure that the mesh was sufficiently fine with 400 elements were carried out by repeating some of the flow calculations using 1600 elements. From the resulting nodal velocity vector, the rivulet flowrate and kinetic energy were calculated from equations

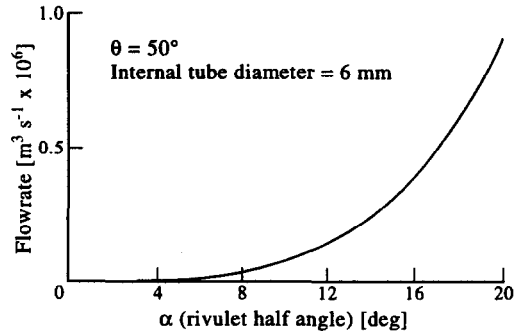

Fig. 3. Effect of changing angle α on rivulet flowrate.

(14) and (16). The variation of the calculated rivulet flowrates and kinetic energies, for this system as a function of the rivulet half angle α, are shown in Figs. 3 and 4.

Once the functions $f(\alpha)$ and $E_K(\alpha)$ have been calculated, the energy vs flowrate curves may be found from equations (21) and (22). A value of n is chosen. Then, from the known value of θ and selected value of α, the quantities β and S are found. The values of E_K and f for the selected value of α are found by interpolation of the data set used to construct the graphs of Figs. 3 and 4.

The values of n, E_K, γ_{lg}, β, S, R, θ, α and f are substituted into equations (21) and (22) to give values of the energy, $E_T - 2\pi R\gamma_{sl}$ and total flowrate F. New values of α are chosen and the new values of relative energy and total flowrate are calculated. As in the film calculations, the pairs of values for energy and flowrate are plotted on a graph.

New values of n are then chosen and the corresponding energy-flowrate curves are constructed. For the plastic tube water system presently under consideration, the graph of Fig. 5 results. The property values used for water (100°C) in these calculations were $\rho = 958.12$ kg m^{-3}, $\mu = 283.1$ μNs m^{-2} and $\gamma_{lg} = 58.78$ mN m^{-1}. In order to make this graph easier to read, only the configurations containing odd numbers of rivulets are shown. It can be seen from this graph that configurations containing more than 15 rivulets would be expected to have energies much

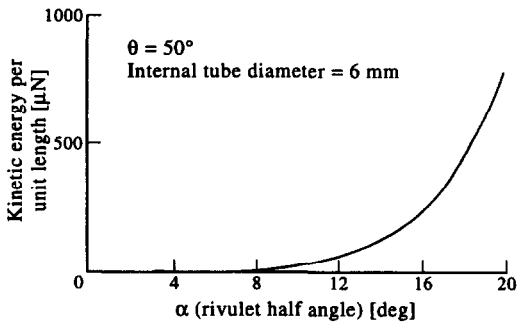

Fig. 4. Effect of changing angle α on rivulet kinetic energy.

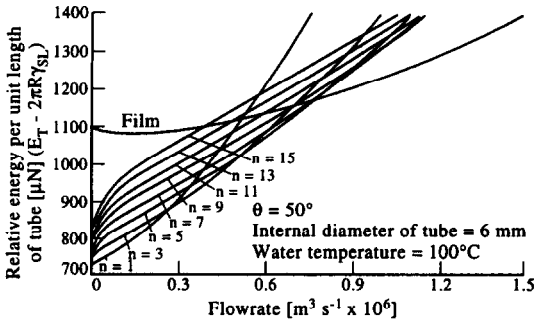

Fig. 5. Relative energy vs flowrate for specified conditions.

Table 1. Values of critical film thickness from three models

θ Contact angle (degrees)	δ_* (μm) Exact calc. for tube (this paper)	Approx. calc. for tube [8]	Plane wall [3]
30	122	127	128
50	157	162	156
70	182	186	177

higher than any of the ground state configurations over the range of flowrates considered.

For flowrates above approximately 0.8×10^{-6} m^3 s^{-1} the film has the lowest energy and will therefore be the favoured configuration. As the flow is reduced from $\sim 0.8 \times 10^{-6}$ m^3 s^{-1} towards zero, the number of rivulets making up the ground state configuration decreases.

A graph of the type shown in Fig. 5 was constructed for two further plastic–water contact angles, $\theta = 30$ and 70°. From these graphs the variation of the critical film thickness δ_* (the thinnest film it is possible to sustain) with contact angle is calculated. The results of these numerical calculations are shown in Table 1 and they are compared to the critical film thicknesses obtained for the same system using the approximate model previously presented by the authors. Also shown in the table are the values of δ_* for 100°C water films travelling down a plane wall using the model of Mikielewicz and Moszynski [3].

The present model is also used to calculate the critical flowrates (the film flowrates when $\delta_0 = \delta_*$) and the rivulet configurations that would be expected to exist if the flow were reduced to just below the critical flowrate. The results of these calculations are shown in Table 2. It can be seen that, for rivulet configurations that exist at flowrates just below the critical flowrate, the ratio of wetted tube area to total tube area is in the range 0.36–0.4.

3.2. *Calculation of heat transfer*

Once the fluid geometry that is expected to exist at each flowrate has been calculated, the associated heat transfer coefficients for the systems may be calculated.

3.2.1. *Film heat transfer.* In order to calculate the overall heat transfer for coefficients for the evaporator, the equation

$$\frac{1}{r}\frac{\mathrm{d}}{\mathrm{d}r}\left(kr\frac{\mathrm{d}T}{\mathrm{d}r}\right) = 0 \tag{23}$$

is solved for the plastic tube–water film system, where the tube of thermal conductivity k_w spans the radial distances R and $R+\delta_w$. The falling film of thermal conductivity k_l extends from $R-\delta_0$ to R. A condensing heat transfer coefficient h exists on the outer surface of the tube wall at $R+\delta_w$.

If an overall heat transfer coefficient U is defined in terms of the inside surface area of the tube ($2\pi R \times$ tube length), then it follows from equation (23) that the overall heat transfer coefficient for the system U is given by

$$U = \left[\left(\frac{R}{R+\delta_w}\right)\frac{1}{h} + \frac{R}{k_w}\ln\left(\frac{R+\delta_w}{R}\right) + \frac{R}{k_l}\ln\left(\frac{R}{R-\delta_0}\right)\right]^{-1}. \tag{24}$$

For the plastic tube evaporator presently under consideration, $R = 3$ mm, $k_w = 0.3$ Wm^{-1} K^{-1} and $k_l = 0.681$ Wm^{-1} K^{-1}. The condensation outside the tube is dropwise and an appropriate value of h is approximately 55 000 Wm^{-2} K^{-1}. With these data, the overall coefficient for the system may be calculated as a function of the film thickness δ_0 (and hence as a function of the film flowrate).

3.2.2. *Rivulet heat transfer.* The equation

$$\frac{\partial^2 T}{\partial x^2} + \frac{\partial^2 T}{\partial y^2} = 0 \tag{25}$$

is solved using the finite element method for the sector in which there is water in contact with the tube. A

Table 2. Critical conditions

Contact angle θ (degrees)	Number of rivulets formed	Half angle of rivulets (°)	Wetted to total tube area, X	Critical flowrate (m^3 s^{-1} x 10^6)
30	4	16.4	0.36	0.36
50	6	11.9	0.4	0.77
70	7	9.4	0.37	1.19

schematic diagram of the system is shown in Fig. 6. As in the fluid flow section, the domain is meshed with triangular elements and the code used for solution was written in FORTRAN.

A condensing heat transfer coefficient h was present on the outside surface of the tube with an associated external temperature of T_0. The nodes on the rivulet free surface were fixed to a temperature $T_0 - \Delta T$.

The tube wall and water had thermal conductivities k_w and k_l, respectively. For the plastic tube evaporator under study ΔT took the value 0.52°C. A value of α was chosen to define the geometry and equation (25) was solved over the domain. From the nodal temperature solution vector, the heat flow Q passing through the tube wall was calculated. A heat transfer coefficient $U_X(\alpha)$ for the part of the tube in contact with the water was then found by dividing the heat flow Q by both the overall temperature difference ΔT and the wetted area of the tube. Use of the inside area of the tube to define the coefficients ensured consistency with the procedures used to find the overall heat transfer coefficients for the falling film system.

The heat transfer performance of the whole tube, including the non-wetted parts, was then obtained by evaluating an overall heat transfer coefficient for the system U from the equation

$$U = U_X \left[\frac{2n\alpha}{360}\right] \tag{26}$$

where α is the rivulet half angle expressed in degrees and n is the number of (congruent) rivulets in the tube.

3.3. *The variation of the heat transfer coefficients with flowrate*

The change in heat transfer performance of the plastic tube evaporator discussed in the previous sections was obtained by first calculating the geometry of the ground state flow configurations that were expected to exist across the flowrate range. Once the geometries of the flows were established, the associated heat transfer properties were calculated.

The results obtained using this procedure are shown in Fig. 7. The graph displayed shows the dependence of U on flowrate for film and rivulet flow (with $\theta = 30$, 50 and 70°). It can be seen that, for each contact angle as the flow is reduced from a stable film condition to a flow just below critical, there is a large reduction in the value of the heat transfer coefficient. Also, it can be seen that the critical flowrate reduces as the contact angle decreases.

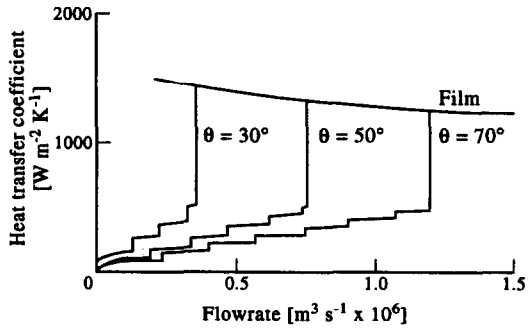

Fig. 7. Theoretical coefficients for film and rivulet flow.

The experiments performed with the plastic tube evaporator correspond to the situation in which $\theta = 50°$. A comparison of the experimental and calculated coefficients is presented in Fig. 8. At the highest experimental flowrate the film Reynolds number was 2300 and, in the tests, the amount of water evaporated in the tube was always less than 2.5% of the flow introduced at the top of the tube [8].

From the graph it can be seen that there is good agreement between experiment and theory for film flows above 2×10^{-6} m^3 s^{-1}. The model correctly predicts a reduction in heat transfer coefficient as the flow reduces to zero. However, the experimental coefficients display a gradual decrease to zero from approximately 2×10^{-6} m^3 s^{-1} whereas the calculated coefficients display a step change at a critical flowrate of 0.77×10^{-6} m^3 s^{-1}. It is possible that this discrepancy arises because the real flows do not always remain in the ground state configuration. It may be that for flows in the range of $0.5\text{–}2 \times 10^{-6}$ m^3 s^{-1} that the energy differences between rivulet and film configurations are low enough to allow transition between states. This would give rise to a gradual rather

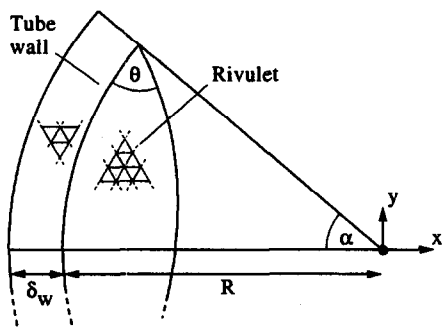

Fig. 6. Finite element system for heat transfer calculations.

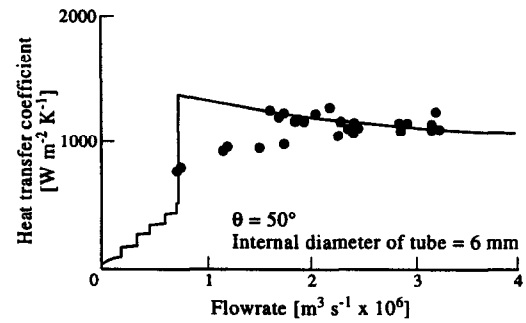

Fig. 8. Theoretical and experimental heat transfer coefficients.

than sudden change in the heat transfer–flowrate function.

3.4. *Generalised model for fluid flow*

The fluid flow calculations for the plastic tube evaporator were performed with the assumption that if there were more than one rivulet in the tube, then each rivulet would have the same geometry. This assumption is not required. The first stage of a generalised calculation sequence requires calculation of the two functions $E_K(\alpha)$ and $f(\alpha)$. After this, an upper limit to the number of rivulets in the tube (P) is chosen together with an upper limit to the rivulet half angle (α_{max}). The angle range 0 to α_{max} is then suitably discretised with M values of α (including zero).

With a maximum of P rivulets which may adopt any of M angle values, it can be shown [8] that the number of distinct flow configurations Z is given by

$$Z = \frac{(M+P-1)!}{P!(M-1)!}. \tag{27}$$

The generalized procedure requires the evaluation of the total energy and flowrate of each of the Z configurations using equations (19) and (20). The configurations are then sorted into narrow bands of flowrate. In each of these bands, an energy corresponding to the film flow configuration must also be provided. The configurations in each flow rate band are then sorted by energy and the geometry adopted over each flow band is taken to be the one with the lowest energy. A more detailed account of this procedure has previously been presented by the authors [8].

4. DISCUSSION

A model has been developed which enables the geometry of fluids travelling down either the inside or outside of vertical tubes to be calculated. This model will be useful in the analysis of many plant processes. A significant advantage of the theory is that the type of flow adopted by the system can be calculated at any flowrate. Once the flow geometry of the system is known, then the associated heat and mass transfer conditions can be calculated. It is expected that this theory will be of value in many plant optimisation studies in which wettability effects are important.

The flow configuration that the system adopts is decided by calculating the total energy of all the possible flow configurations in which the system can exist. At a given flowrate, the system is assumed to adopt the configuration with the lowest energy. However, it should be noted that there may be occasions when the system is not able to adopt the lowest energy configuration.

Consider a group of n rivulets in their ground state travelling down a tube in which the rivulet flow is diminishing because of evaporation. At some point down the tube, if the tube is long enough, calculations will show that the lowest energy state will be provided by a system of $n-1$ rivulets. In this case however, it will not be possible for the $n-1$ rivulet system to form and the system will continue in a higher energy configuration.

There may be other situations in which the system is not able to adopt the lowest energy configuration. Further work is needed to investigate whether systems can in fact adopt their minimum energy configurations.

When the results from the plastic tube evaporator were compared with results from the model, it was found that the experimental heat transfer coefficients varied smoothly with flowrate and did not exhibit a sudden change between film flow and rivulet flow. A closer agreement between the model calculations and the experimental data could probably be obtained by assuming that there may be circumstances in which the system can exist in excited states.

This model is applicable to all surface materials and once the liquid viscosity, density and surface tension are known, it only remains for a measurement of the surface–liquid contact angle to be made. The model described in this paper has been developed from an approximate theory previously presented by the authors. It can be seen from Table 1 that the approximations made were reasonable for the systems considered. The approximate values of δ_* were found to be within 5% of the exact values over the contact angle range 30–70°.

REFERENCES

1. Hartley, D. E. and Murgatroyd, W., Criteria for the break-up of thin liquid layers flowing isothermally over solid surfaces. *International Journal of Heat and Mass Transfer*, 1964, **7**, 1003–1015.
2. Hobler, T., Minimal surface wetting. *Chemia Stosow*, 1964, **2B**, 145 (in Polish).
3. Mikielewicz, J. and Moszynski, J. R., Minimum thickness of a liquid film flowing vertically down a solid surface. *International Journal of Heat and Mass Transfer*, 1976, **19**, 771–776.
4. Allen, R. F. and Biggin, C. M., Longitudinal flow of a lenticular liquid filament down an inclined plane. *The Physics of Fluids*, 1974, **17**(2), 287–291.
5. Towell, G. D. and Rothfeld, L. B., Hydrodynamics of rivulet flow. *A.I.Ch.E. Journal*, 1966, pp. 972–980.
6. Doniec, A., Flow of a laminar liquid film down a vertical surface. *Chemical Engineering Science*, 1988, **43**(4), 847–854.
7. Schmuki, P. and Laso, M., On the stability of rivulet flow. *Journal of Fluid Mechanics*, 1990, **215**, 125–143.
8. Hughes, D. T. and Bott, T. R., The breakup of falling films inside small diameter tubes. *Chemical Engineering Science*, 1991, **46**(7), 1795–1805.
9. Hughes, D. T., Bott, T. R. and Pratt, D. C. F., Plastic tube heat transfer surfaces in falling film evaporators. *2nd U.K. National Heat Transfer Conference*, Glasgow, 1988, pp. 1101–1113.
10. Pratt, D. C. F., The Courtaulds desalination process. *Desalination*, 1982, **42**, 37–45.
11. Pratt, D. C. F., Evaporators, European Patent EP0159885 A2, 1985.
12. Zienkiewicz, O. C., *The Finite Element Method*. McGraw-Hill, New York, 1977.
13. Israelachvili, J., *Intermolecular and Surface Forces*, 2nd edn, Chapter 15. Academic Press, New York, 1991.
14. Jaycock, M. J. and Parfitt, G. D., *Chemistry of Interfaces*, Chapter 5. Ellis Horwood, 1981.